*Int. J. Electrochem. Sci.*, 15 **(2020)** 4619 – 4630, doi: 10.20964/2020.05.79

International Journal of
ELECTROCHEMICAL
SCIENCE
www.electrochemsci.org

# Fabrication of novel electrochemical sensor based on MXene/MWCNTs composite for sensitive detection of synephrine

*Meng Gao*[1], *Yu Xie*[2], *Wuliang Yang*[1,*], *Limin Lu*[2,*]

[1] Key Laboratory of Modern Preparation of TCM of Ministry of Education, College of Traditional Chinese Medicine, Jiangxi University of Traditional Chinese Medicine, Nanchang 330045, PR China
[2] Key Laboratory of Crop Physiology, Ecology and Genetic Breeding, Ministry of Education, College of Science, Jiangxi Agricultural University, Nanchang 330045, PR China
[*]E-mail: jxutcm_zyx@126.com, lulimin816@hotmail.com

*Received:* 29 December 2019 / *Accepted:* 21 February 2020 / *Published:* 10 April 2020

In this study, the composite of MXene/multi-wall carbon nanotube (MXene/MWCNTs) was prepared and utilized to construct electrochemical sensor for detecting synephrine. The MXene/MWCNTs material has both the advantages of MXene and MWCNTs, including large electrochemically active surface, good physical and chemical properties of MXene, and high electrical conductivity as well as excellent electrocatalytic activity of MWCNTs. These excellent properties ensure high sensitivity. In addition, the structure of the material was characterized by scanning electron microscope (SEM) and X-ray diffraction (XRD). The application of the modified electrode was studied by cyclic voltammetry (CV) and linear sweep voltammetry (LSV). Under optimized experimental conditions, a linear relationship between the peak current and the concentration of synephrine was established in the range of 0.5 ~ 70 μM. A low limit of detection of 0.167 μM was obtained. The modified electrode also showed good repeatability, stability and anti-interference ability.

**Keywords:** MXene; MWCNTs; Electrochemical sensor; Synephrine.

## 1. INTRODUCTION

Synephrine is an alkaloid in various plants such as tangerine peel and citrus, which is widely used in the pharmaceutical, food, beverage, feed and cosmetics industries [1]. In 2004, the US FDA approved its replacement for ephedrine for dietary supplements and applied to weight loss products. Synephrine has various pharmacological effects, such as preventing excess energy (heat accumulation), regulating qi by wind, increasing blood pressure, promoting appetite and accelerating metabolism [2]. It is also a mild fragrant expectorant, a neurotranquilizer and a laxative for

constipation. In addition to the traditional application in traditional Chinese medicine, its injection can be used to rescue various shock, heart failure and treatment of gastric and duodenal ulcer and other diseases [3]. However, it has been reported that synephrine has potential side effects and even toxicity on cardiovascular system [4]. In 2010, Health Canada recommended that the daily dose of synephrine should be less than 30 mg [5]. Therefore, accurate detection of the content of synephrine in medicine or food health care products is beneficial to give advice on the maximum dosage.

Up to now, liquid chromatography tandem mass spectrometry (LC-MS/MS) [6], capillary electrophoresis [7], fluorescence [8], electrospray ionization mass spectrometry (ESI-MS) [9] and high performance liquid chromatography (HPLC) [10] have been developed for the detection of synephrine. Compared with these conventional methods, electrochemical methods have the advantages of simplicity, low cost, fast response and high sensitivity [11,12]. For electrochemical sensor, the detection sensitivity mainly relies on electrode material.

MXene, a two-dimensional layered early transition metal carbide and carbonitride has attracted extensive attention due to its large electrochemically active surface, intriguing physical and chemical properties and hydrophilic surface [13]. It has been widely used in electrochemical fields. For example, Zhang group designed MXene modified screen-printed electrode for simultaneous voltammetric determination of acetaminophen and isoniazid [14]. Zhou group constructed a biosensor based on acetylcholinesterase/MXene composite for organophosphate oesticides determination [15]. Zheng group prepared an inkjet print MXene-graphene oxide electrode for electrochemical detection of $H_2O_2$ [16]. Although MXene has so many advantages, the serious agglomeration of MXene affects its electrochemical performance. Therefore, effective prevention of MXene aggregation is the key to improve its sensing performance.

Multi-walled carbon nanotubes (MWCNTs) are widely used in electrochemistry owing to their unique one-dimensional (1D) structural, mechanical and electronic properties [17]. Recent research indicates that MWCNTs as spacer can effectively prevent the agglomeration of MXene and greatly improve the catalytic activity of the composite. For instance, Cai group fabricated ultrasensitive strain sensor based on stretchable $Ti_3C_2T_x$ MXene/carbon nanotube composite [18]. Huang group achieved the simultaneously electrochemical determination of hydroquinone and catechol with the use of self-assembled $Ti_3C_2$/MWCNTs electrode material [19]. These works demonstrate that MXene /MWCNTs hybrid is an ideal electrode material for electrochemical sensor. However, yet there is no report on MXene/MWCNTs hybrid as the electrode material for the detection of synephrine.

Herein, this study reported the utilization of MXene/MWCNTs electrode for the determination of synephrine. The composite of Mxene and MWCNTs with three-dimensional interconnection structure, has good conductivity and rich active sites, which is beneficial to the electrochemical detection of simephrine. Based on these advantages of composite materials, good sensing performances have been achieved with a wide liner range of 0.5 ~ 70 μM and limit of detection (LOD) of 0.167 μM. The designed sensor was also successfully employed for simephrine detection in fructus aurantii samples.

## 2. EXPERIMENT

### *2.1. Chemicals and instruments*

MXene and MWCNTs were bought from XF NANO, INC (Nanjing, China). Synephrine, N, N-dimethyllformamide (DMF), $Na_2HPO_4$ and $NaH_2PO_4$ were shopped from Aldrich Co. Ltd (Shanghai, China). Phosphoric acid buffer solution (PBS) with different pH value was prepared by mixing 0.1 M $Na_2HPO_4$ and $NaH_2PO_4$.

The morphologies of MXene and MXene/MWCNTs were observed by Zeiss 40 scanning electron microscope. XRD patterns were obtained on Bruker D8 diffractometer. All electrochemical data were tested on the CHI 760E electrochemical workstation. The saturated calomel electrode is a reference electrode, the platinum electrode is anode electrode, and bare electrode (GCE, $\Phi$= 3 mm) or the modified electrode is cathode electrode.

### *2.2. Preparation of the modified electrodes*

10 mg MXene and 10 mg MWCNTs were dispersed in 10 mL DMF to obtain 1.0 mg $mL^{-1}$ MXene dispersion and 1.0 mg $mL^{-1}$ dispersion, respectively. MXene/MWCNTs composite dispersion was prepared via dispersing 10.0 mg MXene and 10.0 mg MWCNTs into 10 mL DMF with following sonication for 1 h.

Bare glassy carbon electrode (GCE) was polished with suede. It was ultrasonically washed several times with water and ethanol until the surface is mirrored. 5.0 μL of MXene, MWCNTs and MXene/MWCNTs dispersions were then dropped on GCEs, respectively. After that, these modified GCE were dried under infrared light to form MXene/GCE, MWCNTs/GCE and MXene/MWCNTs/GCE.

### *2.3. Measurement procedure*

The modified GCEs were inserted in PBS (pH 7.0) for CV scanning under the potential ranging from 0.2 to 1.0 V, and LSV scanning ranging from 0.3 to 1.0 V. Electrochemical impedance spectroscopy (EIS) was measured in 0.1 M KCl containing 5.0 mM $[Fe(CN)_6]^{3-/4-}$ with the initial potential of 0.25 V and the frequency of 0.1 ~ 10 kHz. Chronocoulometry analysis was conducted in 1.0 M KCl containing 0.1 mM $K_3[Fe(CN)_6]$.

## 3. RESULTS AND DISCUSSION

### *3.1. Characterization of MXene and MXene/MWCNTs*

SEM images of MXene (A) and MXene/MWCNTs (B) were shown in Fig. 1. As presented in Fig. 1A, MXene has a sheet-like structure and resembles an accordion, indicating that MXene layer has a large specific surface area, which is beneficial to the adsorption of synephrine. From Fig. 1B, it

can be seen that some MWCNTs are attached on the surface of MXene and some are inserted into the layer of MXene sheets, demonstrating three-dimensional interconnected structure.

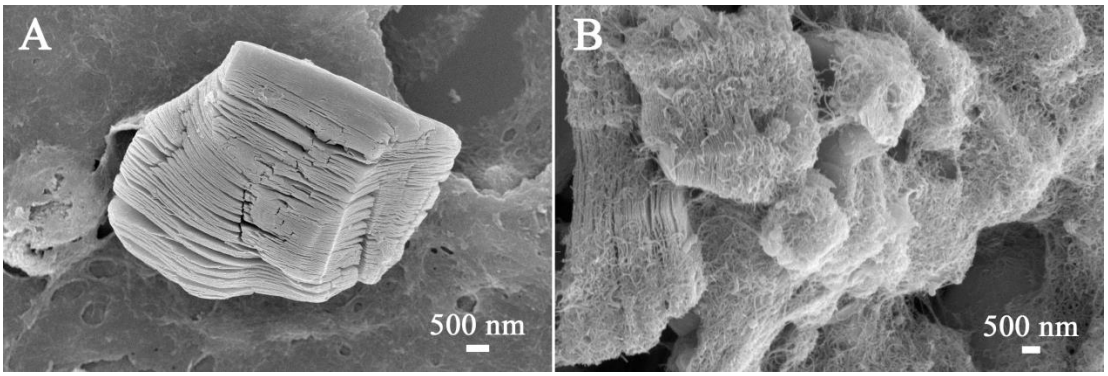


**Figure 1.** SEM images of MXene (A) and MXene/MWCNTs (B).

EIS spectrum was used to investigate the charge transfer resistance ($R_{ct}$) of modified materials [20]. The semicircle diameter of the low frequency part represents $R_{ct}$. Fig. 2 depicts the EIS spectrums of various modified electrodes. The $R_{ct}$ of MXene/GCE (b) and MWCNTs/GCE (c) were smaller than that of bare GCE (a), indicating that MXene and MWCNTs can enhance charge transfer. For MXene/MWCNTs/GCE (d), the semicircle diameter decreased sharply compared with bare GCE (a) and MXene/GCE (b), suggesting that MWCNTs improved the agglomeration of MXene, and thus the conductivity of composite was enhanced.

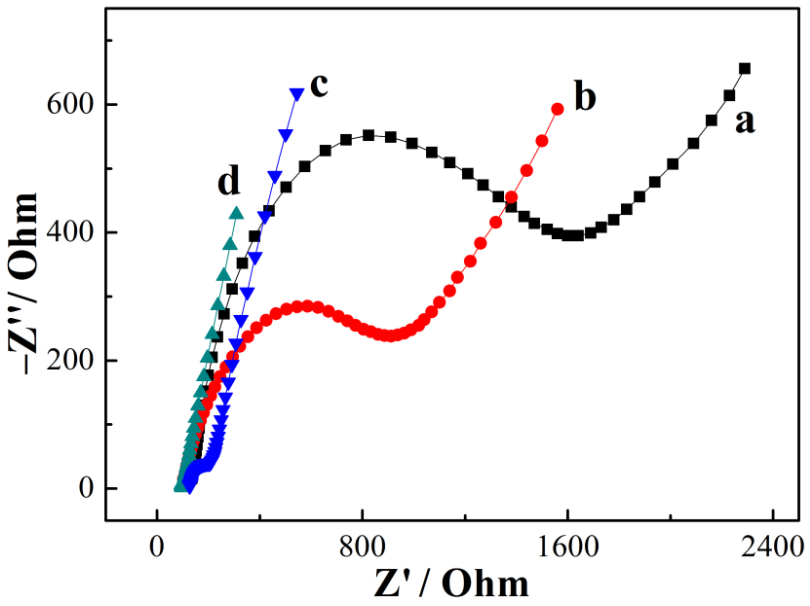


**Figure 2.** EIS plots of bare GCE (a), MXene/GCE (b), MWCNTs/GCE (c) and MXene/MWCNTs/GCE (d) in a solution containing 5 mM $[Fe(CN)_6]^{3-/4-}$ and 0.1 M KCl with the frequencies from 0.1 to 10000 Hz; Potential: 0.25 V; Amplitude: 0.005 V.

### *3.2. Chronocoulometry*

The effective surface area of different modified electrode (Fig. 3A) can be calculated by the Anson equation [21]:

$Q(t) = 2nFAcD^{1/2}t^{1/2}/\pi^{1/2} + Q_{dl} + Q_{ads}$

Where, $Q_{dl}$ is double layer charge, $Q_{ads}$ is Faradic charge. n is known as the electrons transferred number, F is mentioned as Faraday constant, and c knows as the reactant concentration [22]. D represents the diffusion coefficient. The Q-$t^{1/2}$ plots of bare GCE (a'), MWCNTs/GCE (b'), MXene/GCE (c') and MXene/MWCNTs/GCE (d') can be expressed as Q ($10^{-6}$ C) = 4.745 + 33.738 $t^{1/2}$ ($R^2$ = 0.999), Q ($10^{-6}$ C) = 7.784 + 51.673 $t^{1/2}$ ($R^2$ = 0.999), Q ($10^{-6}$ C) = 10.718 + 105.215 $t^{1/2}$ ($R^2$ = 0.999) and Q ($10^{-6}$ C) = 60.902 + 159.069 $t^{1/2}$ ($R^2$ = 0.999), respectively (Fig. 3B). According to the slope of Q-$t^{1/2}$ curves, the effective surface areas of the corresponding electrodes were estimated to be 0.113, 0.0.172, 0.351 and 0.531 $cm^2$, respectively. The large specific surface area of MXene/MWCNTs/GCE offered sufficient active sites for the electro-oxidation reaction of synephrine, resulting in the enhancement of electrochemical performance.

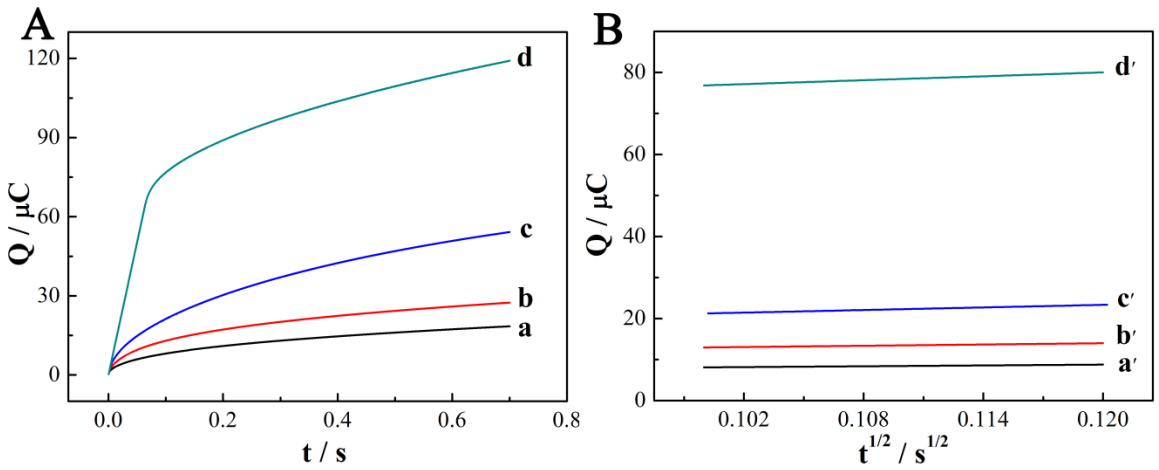


**Figure 3.** (A) Q-t plots of bare GCE (a), MWCNTs/GCE (b), MXene/GCE (c) and MXene/MWCNTs/GCE (d). (B) Q-$t^{1/2}$ plots of bare GCE (a'), MWCNTs/GCE (b'), MXene/GCE (c') and MXene/MWCNTs/GCE (d').

### *3.3. Electrochemical behaviors*

The electrochemical behaviors of 10 μM synephrine at different modified electrodes were explored by CV in 0.1 M PBS (pH 7.0). From Fig. 4, there were no peaks on bare GCE. While, a weak anodic peak was observed on MXene/GCE, which was due to the good conductivity of MXene. At MWCNTs/GCE, significant oxidation peak appeared owing to the excellent electron transfer and catalytic properties of MWCNTs. Moreover, in comparison with that at MWCNTs/GCE, a remarkable increase in oxidation current was observed at MXene/MWCNTs/GCE. The phenomenon was ascribed to the fact that the incorporation of MWCNTs into MXene avoided the aggregation of MXene, which

improved the mass transport capacity, conductivity and excellent electrocatalytic effect towards synephrine.

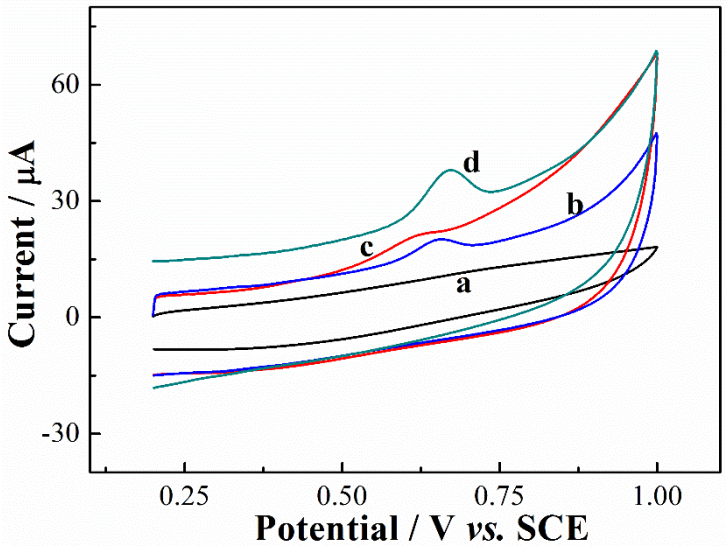


**Figure 4.** CV behaviors of synephrine (10 μM) in 0.1 M PBS (pH 7.0) on bare GCE (a), MWCNTs/GCE (b), MXene/GCE (c) and MXene/MWCNTs/GCE (d). Accumulation time: 120 s. Scan rate: 100 mV $s^{-1}$.

### *3.4. Optimizations of parameters*

In order to improve the sensitivity of MXene/MWCNTs/GCE, some experimental conditions including the volume of MXene/MWCNTs and the accumulation time were optimized. Fig. 5 shows the effect of MXene/MWCNTs volume and accumulation time on LSV response toward 10 μM synephrine. As can be seen from Fig. 5A, the LSV response increased as the modification volume increased from 1.0 to 5.0 μL, but decreased after exceeding 5.0 μL. This phenomenon was owing to the fact that the too thick MXene/MWCNTs film on the electrode surface hindered the mass transfer [23]. Thus, 5.0 μL was chosen for the fabrication of MXene/MWCNTs/GCE.

In Fig. 5B, the LSV response strengthened as the accumulation time increased, and reached the plateau after 120s, which was due to the saturated adsorption of simephrine on the electrode surface. So, 120 s was applied for the following experiments.

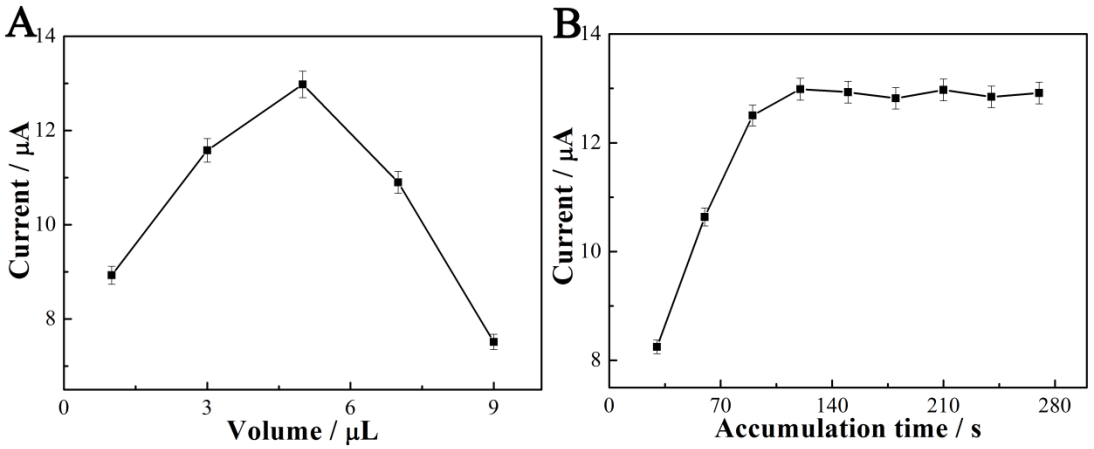


**Figure 5.** Effects of (A) the MXene/MWCNTs volume and (B) the accumulation time to the LSV response of 10 μM synephrine at MXene/MWCNTs/GCE.

### *3.5. Effects of pH and scan rates*

The influence of the solution pH on the peak current was investigated by CV. Fig. 6A displays that the current response increased from pH 5.0 to 7.0. While, the response reduced when pH value raised from 7.0 to 9.0. Thus, pH 7.0 was adopted for the electrochemical determination of synephrine. From Fig. 6B, there was a linear relationship between peak potential ($E_{pa}$) and pH. The equation was expressed as $E_{pa}$ = 1.130 – 0.065 pH ($R^2$ = 0.998). The slope of the equation was -0.065 V $pH^{-1}$, which is close to the theoretical value of -0.059 V $pH^{-1}$, implying that the number of electron transfer was equal to the number of proton participating in the reaction [24].

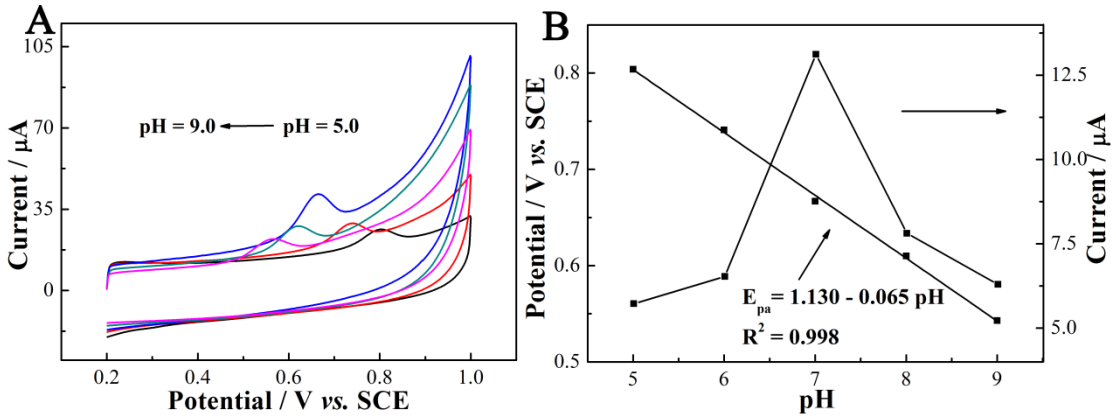


**Figure 6.** (A) CVs of 10.0 μM synephrine at MXene/MWCNTs/GCE in 0.1 M PBS with different pH value (5.0, 6.0, 7.0, 8.0, 9.0). (B) Effect of pH value on the peak potential and peak current.

The CV profiles of the MXene/MWCNTs/GCE at different scan rates ($v$) from 10 to 300 mV $s^{-1}$ are depicted in Fig. 7A. The CV response was linear with the scan rates (inset of Fig. 7A), and the corresponding equation was I = 2.208 + 0.097 $v$ ($R^2$ = 0.994). The result showed that the electro-oxidation of synephrine on the electrode was an adsorption-controlled process [25]. Moreover, the

relationship of $E_{pa}$ and ln *v* can be fit as $E_{pa}$ = 0.546 + 0.026 ln *v* ($R^2$ = 0.996, Fig. 7B). Based on the Laviron theory [26]:

$$E_{pa} = E^0 - (RT/\alpha nF)\ln(RTk_s/\alpha nF) + (RT/2\alpha nF)\ln v$$

Herein, R, T and F have usual meanings. αn was calculated to be 1.04 based on slope of $E_{pa}$-ln *v* equation. For a totally irreversible electrode process, α is assumed to be 0.5 [27], thus, the electron transfer number n was evaluated to be 2. As the number of electrons in synephrine oxidation process is equal to the number of protons, therefore, therefore, the oxidation process of synephrine at MXene/MWCNTs/GCE involves two-proton and two-electron.

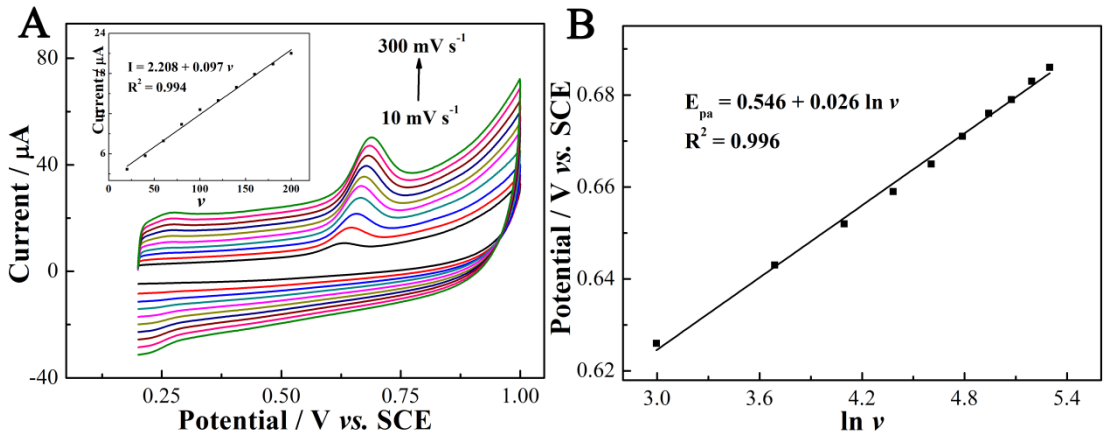


**Figure 7.** (A) CVs of 10 μM synephrine on MXene/MWCNTs/GCE with different scan rates from 10 to 300 mV $s^{-1}$. Inset: plots of I *vs. v*. (B) Plot of E *vs.* ln *v*.

### *3.6. Determination of synephrine*

Fig. 8 shows the LSV plots of different synephrine concentration at MXene/MWCNTs/GCE. As depicted, the LSV response gradually increased as the concentration varied from 0.5 μM to 70 μM. The current value was proportional to the concentration and the relationship can be express as I = 1.382 c – 0.579 ($R^2$ = 0.996). The limit of detection (LOD) of the sensor was calculated to be 0.167 μM (S/N = 3), which was lower than those reported by other methods (Table 1) [27]. Such good performance was due to the synergistic effect of MXene and MWCNTs. The introduction of MXene enlarged the electroactive surface area of the electrode. While, MWCNTs enhanced the electron transfer ability, thus facilitating the rapid mass transfers between the modified electrode and the solution.

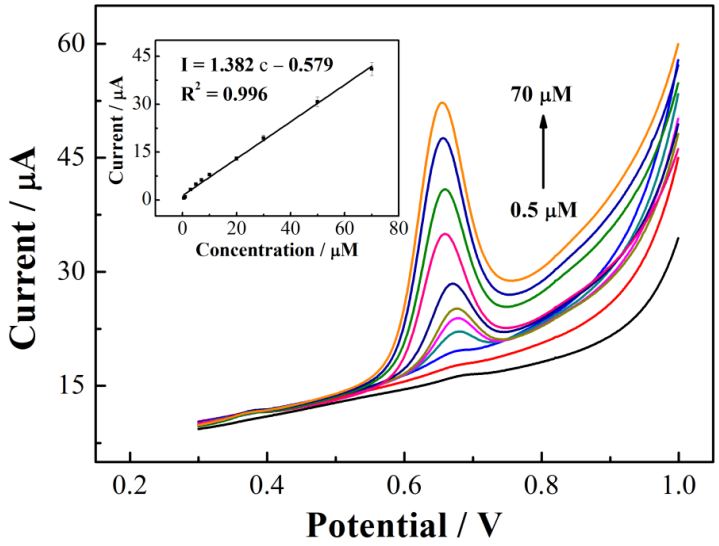


**Figure 8.** The LSV plots of synephrine with different concentrations (0.5, 0.7, 1.0, 3.0, 5.0, 7.0, 10, 20, 30, 50 and 70 μM) at MXene/MWCNTs/GCE in 0.1 M PBS (pH 7.0). Inset: the liner calibration curve.

**Table 1.** Comparison of different methods towards synephrine detection.

| Methods | Liner range | LOD | Reference |
|---|---|---|---|
| Gas chromatography -mass spectrometry | 590 μM -0.299 M | 590 μM | 28 |
| High performance liquid chromatography | 15.25 μM-15.25 mM | 7.236 μM | 29 |
| MXene/MWCNTs/GCE | 0.5 -70 μM | 0.167 μM | This work |

*3.7. Reproducibility, stability and interferences*

To evaluate the reproducibility, nine parallel MXene/MWCNTs/GCEs were used for the detection of 10 μM synephrine. The RSD of the obtained LSV currents was 3.8%, implying good reproducibility.

The MXene/MWCNTs/GCE was stored at room temperature and used to determine 10 μM synephrine every two days. After one month, the current signal remained at 96.4% of the initial value, indicating that the electrode has satisfactory stability.

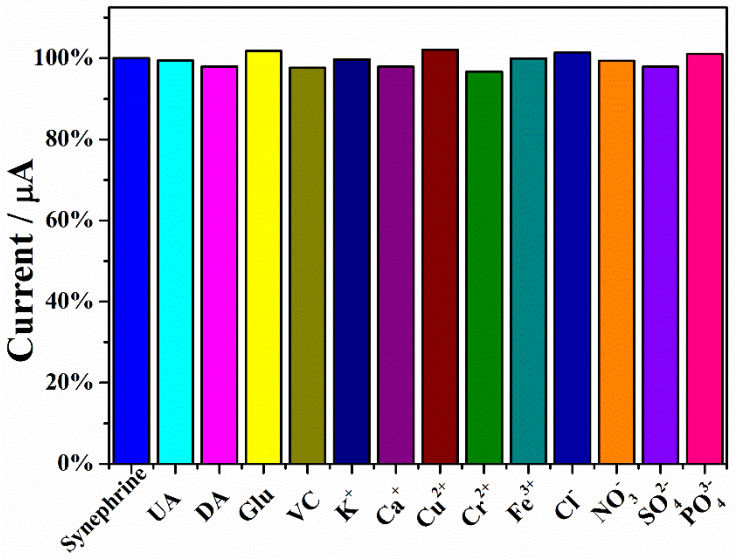


**Figure 9**. Interference study: DPV results of MXene/MWCNTs/GCE in 10 μM synephrine, and the mixture of 10 μM synephrine and 10 μM uric acid (UA), dopamine (DA), glucose (Glu), ascorbic acid (VC) or 0.5 mM different ions, respectively.

Moreover, the selectivity of MXene/MWCNTs/GCE in the presence of 10 μM synephrine and different interference substances was investigated. As depicted in Fig. 9, 50 μM uric acid (UA), dopamine (DA), glucose (Glu), ascorbic acid (VC) and 0.5 mM other ions ($K^+$, $Ca^{2+}$, $Cu^{2+}$, $Cr^{2+}$, $Fe^{3+}$, $Cl^-$, $NO_3^-$, $SO_4^{2-}$ and $PO_4^{3-}$) did not interfere with the detection of 10 μM synephrine (LSV signal changed below 3.30%). The result demonstrated that the sensor presented acceptable selectivity.

### *3.8. Real sample analysis*

To examine the analytical reliability and application of the sensor to real sample, the electrode was applied to detect synephrine in fructus aurantii sample that from different place (Chongqing city, Sichuan province and Jiangxi province in China). 10 g of fructus aurantii powder was added into conical flask with 50 mL of methanol. The solution was heated in a water bath and reflux for 1.5 h. After cooling down, the volume of methanol was kept to be 50 mL. The product was filtered. 10 mL of filtrate was transferred to evaporate, and the obtained product was dissolved in 10 mL water. After flowing through the polyamide column, the above solution was eluted with 25 mL water, the eluant was collected, and the volume was fixed to 25 mL with water.

The above solutions were detected by the proposed sensor and high performance liquid chromatography (HPLC), respectively. As shown in Table 2, the results from our designed method are in good agreement with HPLC method, suggesting that the sensor can be applied for the determination of synephrine in real samples efficiently and accurately.

**Table 2.** Determination of synephrine in fructus aurantii by the electrochemical sensor based on MXene/MWCNTs/GCE (n= 3).

| Fructus aurantii from | sample | by proposed sensor (μg/100 mL) | RSD (%) | by HPLC method (μg/100 mL) | RSD (%) |
|---|---|---|---|---|---|
| Chongqing | 1 | 1.630 | 2.64 | 1.635 | 1.06 |
| | 2 | 1.297 | 1.14 | 1.278 | 3.24 |
| Sichuan | 1 | 1.683 | 4.28 | 1.676 | 4.19 |
| | 2 | 1.710 | 2.13 | 1.724 | 0.69 |
| Jiangxi | 1 | 2.514 | 3.34 | 2.501 | 2.42 |
| | 2 | 3.219 | 1.67 | 3.235 | 1.19 |

## 4. CONCLUSIONS

In summary, a rapid and simple method based on MXene/MWCNTs/GCE was designed for the electrochemical determination of synephrine. Due to the excellent electrocatalytic activity and high conductivity of MWCNTs, large surface area of MXene as well as the synergistic effect between MXene and MWCNTs, the sensor demonstrated wide detection range (0.5 ~ 70 μM) and low limit of detection (0.167 μM) towards synephrine. The sensor was also applied for detect synephrine in fructus aurantii samples, and satisfactory results were obtained.

ACKNOWLEDGEMENTS
We are grateful to the National Natural Science Foundation of China (81760680, 81460575, 21665010 and 51862014) for their financial support of this work.

## References

1. E. Marchei, S. Pichini, R. Pacifici, M. Pellegrini, P. Zuccaro, *J. Pharm. Biomed. Anal.*, 41 (2006) 1468.
2. D. L. Ribeiro, A. R. T. Machado, C. da Silva Machado, P. Santos, A. F. Aissa, G. R. M. Barcelos, L. M. G. Antunes, *Toxicology*, 422 (2019) 25.
3. L. G. Rossato, P. G. de Pinho, R. Silva, H. Carmo, F. Carvalho, L. Bastos Mde, V. M. Costa, F. Remiao, *J. Pharm. Biomed. Anal.*, 52 (2010) 721.
4. S. J. Stohs, *Food Chem. Toxicol.*, 49 (2011) 1472.
5. L. G. Rossato, V. M. Costa, R. P. Limberger, M. de Lourdes Bastos, F. Remião, *Food Chem. Toxicol.*, 49 (2011) 8.
6. M. L. Gay, R. A. Niemann, S. M. Musser, *J. Agric. Food Chem.*, 54 (2006) 285.
7. G. Chen, L. Zhang, J. Zhao, J. Ye, *Anal. Bioanal. Chem.*, 373 (2002) 169.
8. R. A. Niemann, M. L. Gay, *J. Agric. Food Chem.*, 51 (2003) 5630.
9. X. G. He, L. Lian, L. Lin, M. W. Bernart, *J. Chromatogr. A*, 791 (1997) 127.
10. B. Avula, S. K. Upparapalli, A. Navarrete, I. A. Khan, *J. AOAC Int.*, 88 (2005) 1593.
11. Y. Qian, C. Wang, F. Gao, *Biosens. Bioelectron.,* 63 (2015) 425.
12. J. Liu, W. Zhang, Y. Li, L. Yang, B. Ye, *Anal. Methods*, 5 (2013) 5317.

13. Y. Li, Z. Kang, L. Kong, H. Shi, Y. Zhang, M. Cui, D. P. Yang, *Mater. Sci. Eng., C*, 104 (2019) 110000.
14. Y. Zhang, X. Jiang, J. Zhang, H. Zhang, Y. Li, *Biosens. Bioelectron.*, 130 (2019) 315.
15. L. Zhou, X. Zhang, L. Ma, J. Gao, Y. Jiang, *Biochem. Eng. J.*, 128 (2017) 243.
16. J. Zheng, J. Diao, Y. Jin, A. Ding, B. Wang, L. Wu, B. Weng, J. Chen, *J. Electrochem. Soc.*, 165 (2018) B227.
17. X. Qiu, L. Lu, J. Leng, Y. Yu, W. Wang, M. Jiang, L. Bai, *Food Chem*., 190 (2016) 889.
18. Y. Cai, J. Shen, G. Ge, Y. Zhang, W. Jin, W. Huang, J. Shao, J. Yang, X. Dong, *ACS Nano*, 12 (2018) 56.
19. R. Huang, S. Chen, J. Yu, X. Jiang, *Ecotoxicol. Environ. Saf.*, 184 (2019) 109619.
20. Y. Qian, D. Tang, L. Du, Y. Zhang, L. Zhang, F. Gao, *Biosens. Bioelectron.,* 64 (2015) 177.
21. X. Zhu, L. Lu, X. Duan, K. Zhang, J. Xu, D. Hu, H. Sun, L. Dong, Y. Gao, Y. Wu, *J. Electroanal. Chem.*, 731 (2014) 84.
22. F. C. Anson, *Anal. Chem.*, 36 (1964) 93.
23. S. Chen, R. Huang, J. Zou, D. Liao, J. Yu, X. Jiang, *Ecotoxicol. Environ. Saf.*, 191 (2020) 110194.
24. W. Zhang, L. Zong, S. Liu, S. Pei, Y. Zhang, X. Ding, B. Jiang, Y. Zhang, *Biosens. Bioelectron.*, 131 (2019) 200.
25. X. Zhu, K. Zhang, N. Lu, X. Yuan, *Appl. Surf. Sci.*, 361 (2016) 72.
26. J. Li, X. Li, R. Yang, L. Qu, B. Harrington Pde, *Anal. Chim. Acta*, 804 (2013) 76.
27. J. Li, D. Miao, R. Yang, L. Qu, P. d. B. Harrington, *Electrochim. Acta*, 125 (2014) 1.
28. E. Marchei, S. Pichini, R. Pacifici, M. Pellegrini, P. Zuccaro, *J Pharmaceut Biomed.,* 41 (2006) 1468.
29. Y.N. Yi, X. Cheng, L. Liu, G. Hu, Z. Wang, Y. Deng, K. Huang, G. Cai, C.H. Wang, *Pharm Biol.,* 50 (2012) 832.